

Inverse modelling of European N₂O emissions: Assimilating observations from different networks

Supplementary Material

M. Corazza¹, P. Bergamaschi¹, A. T. Vermeulen², T. Aalto³, L. Haszpra⁴, F. Meinhardt⁵, S. O'Doherty⁶, R. Thompson⁷, J. Moncrieff⁸, E. Popa², M. Steinbacher⁹, A. Jordan¹⁰, E. Dlugokencky¹¹, C. Brühl¹², M. Krol¹³, and F. Dentener¹.

[1] European Commission Joint Research Centre, Institute for Environment and Sustainability, I-21027 Ispra (Va), Italy.

[2] Energy research Centre of the Netherlands (ECN), Petten, The Netherlands

[3] Finnish Meteorological Institute (FMI), Finland

[4] Hungarian Meteorological Service, Budapest, Hungary

[5] Umweltbundesamt (UBA), Messstelle Schauinsland, Kirchzarten, Germany

[6] School of Chemistry, University of Bristol, UK

[7] Laboratoire des Sciences du Climat et de l'Environnement (LSCE), Gif sur Yvette, France

[8] Edinburgh University, UK

[9] Swiss Federal Laboratories for Materials Science and Technology (Empa), Duebendorf, Switzerland

[10] Max Planck Institute for Biogeochemistry, Jena, Germany

[11] NOAA Earth System Research Laboratory, Global Monitoring Division, Boulder, CO, USA

[12] Max Planck Institute for Chemistry, Mainz, Germany

[13] Wageningen University and Research Centre (WUR), Wageningen, The Netherlands

October 13, 2010

Corresponding Author Address: Matteo Corazza: matteo.corazza@jrc.ec.europa.eu

Submitted to *Atmos. Chem. Phys.*

Figure Captions

Figure S-1: The 3 two-way nested domains used for all the zoomed simulations presented in this work. Locations of all stations used in the control inversion are also shown. Open circles represent flask measurements, and filled circles are continuous measurements.

Figure S-2: Monthly values for the atmospheric sink rates: Upper panel: reaction with $O(^1D)$, middle panel: photolysis. Values for January, April, July and October are shown to illustrate the seasonal variation. Bottom panel: N_2O mole fractions from the ECHAM model.

Figure S-3: Example of annual evolution of N_2O mole fractions at 8 of the available global stations: Alert, Ny-Ålesund, Barrow, Niwot Ridge, Mauna Loa, Ascension Island, Crozet Island, and South Pole. One year of data, from 1 January to 31 December 2006, is presented. As in Fig. 2, blue lines represent a priori simulations and red lines are a posteriori simulations for the reference inversion S1. Shaded areas represent estimated uncertainties of the model simulations. Measurements are shown as black dots. Latitude, longitude, and height (meters above sea level) are also reported for each station.

Figure S-4: A priori (top panel) and a posteriori (mid panel) annual emissions over the $6^\circ \times 4^\circ$ global domain for 2006 for the reference inversion S1. Bottom panel represents the difference between the two fields (a posteriori – a priori).

Figure S-5: A posteriori annual emissions for sensitivity inversion S2 (top left panel) and S3 (top right panel). In the bottom panels their differences to the reference inversion S1 are shown.

Figure S-6: A posteriori emission distribution for S4 (top panel) and difference to reference inversion S1 (mid panel of Fig. 3).

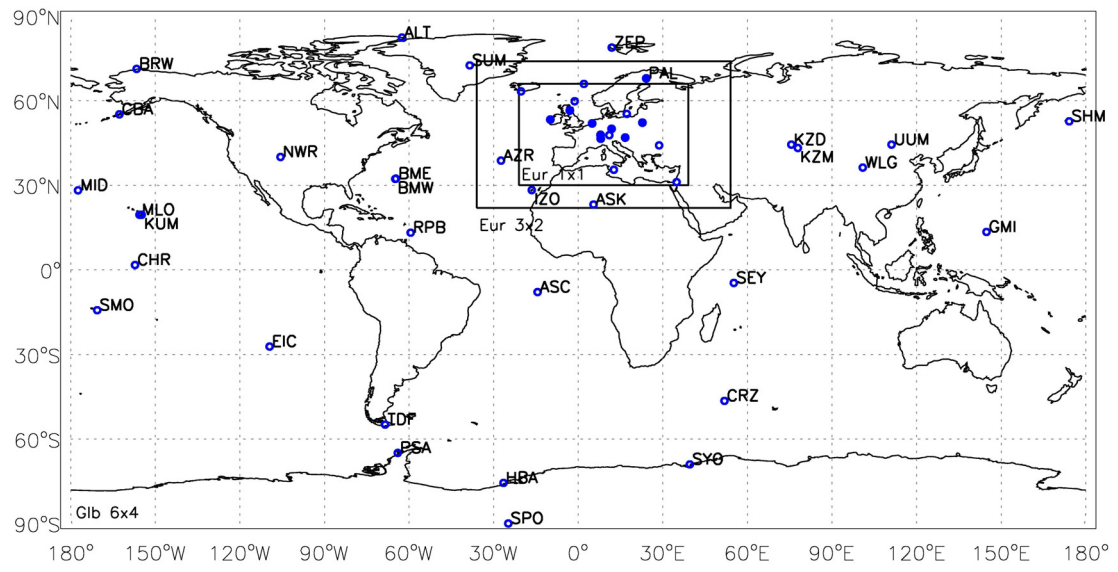


Figure S-1

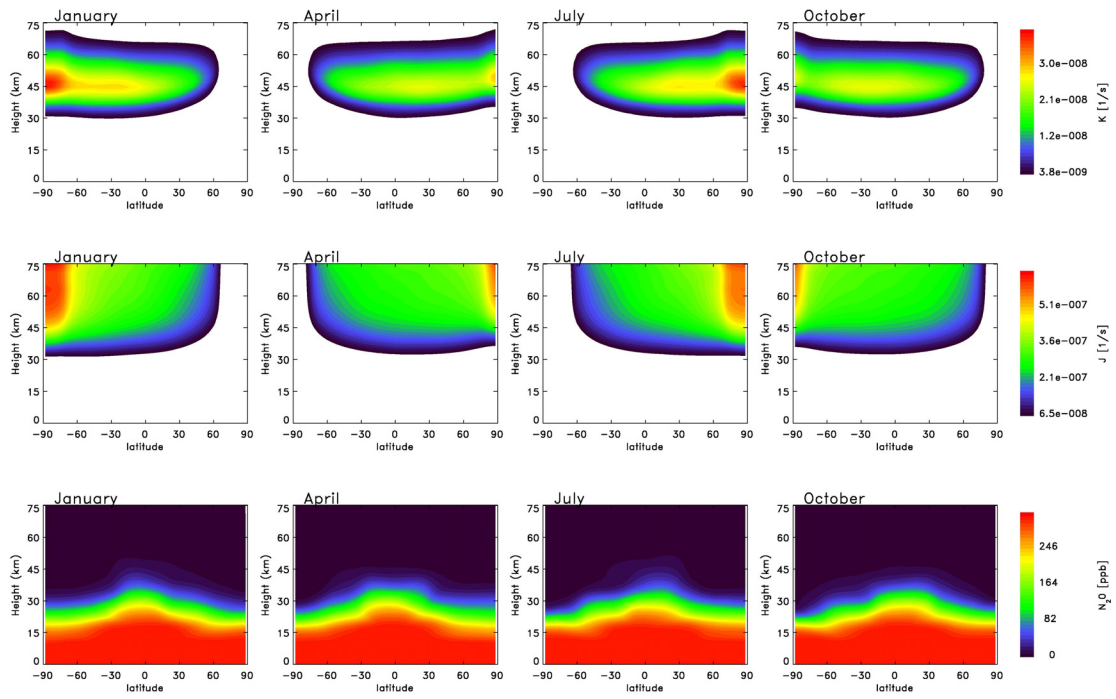


Figure S-2

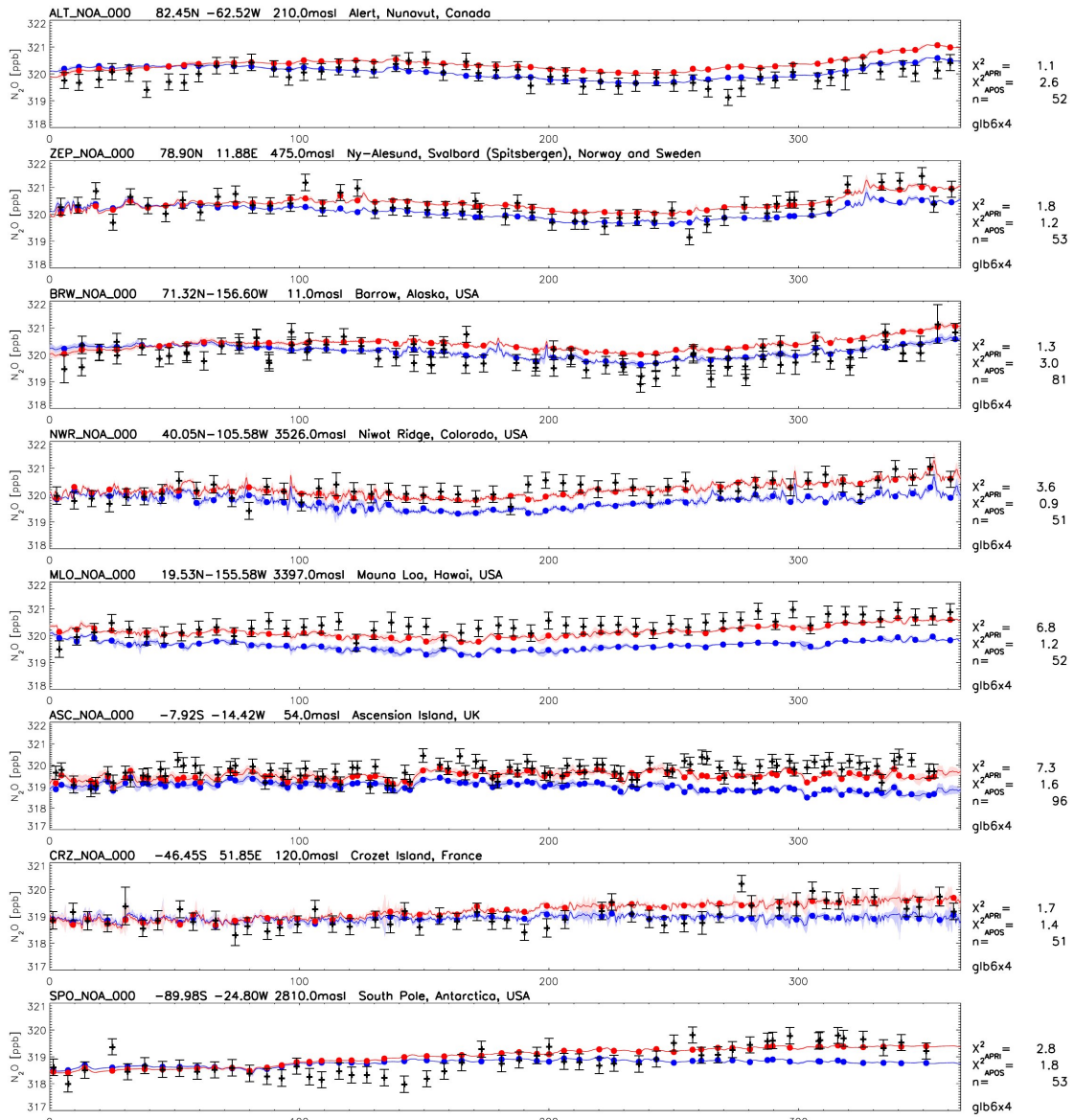
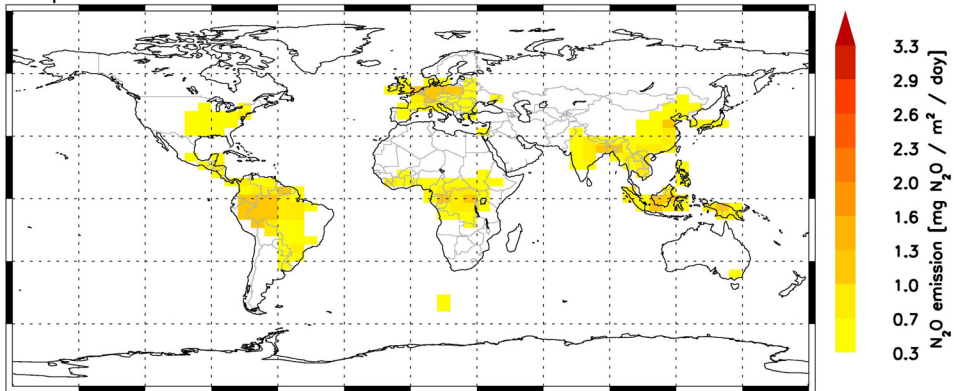


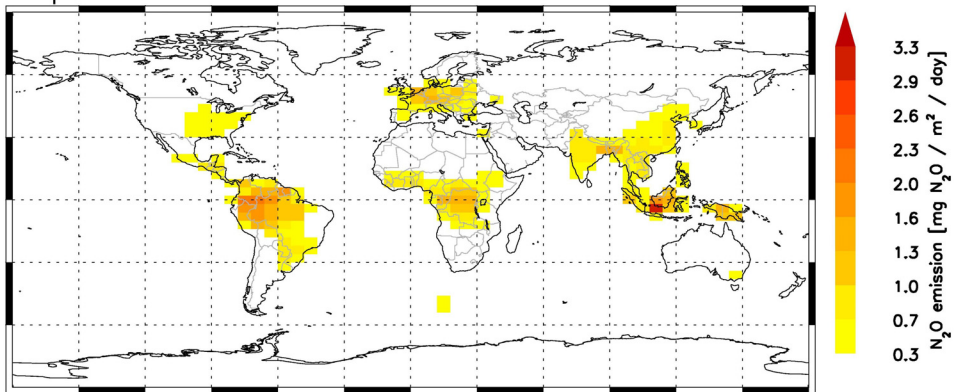
Figure S-3

total emissions
a priori

01 2006 – 12 2006



a posteriori



posteriori – priori

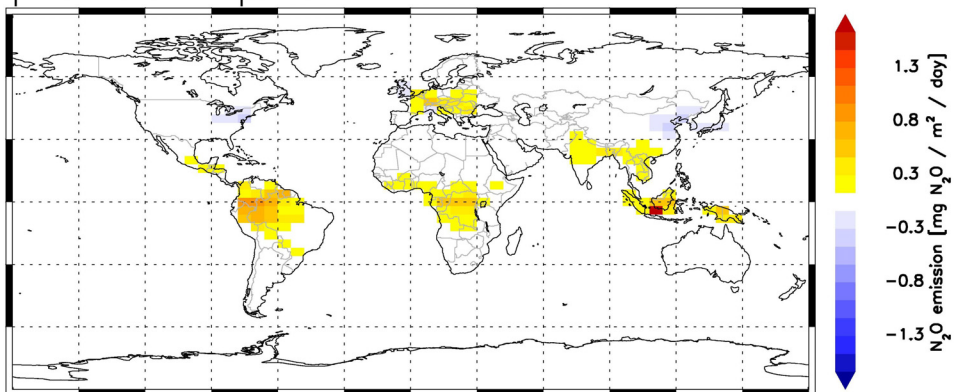


Figure S-4

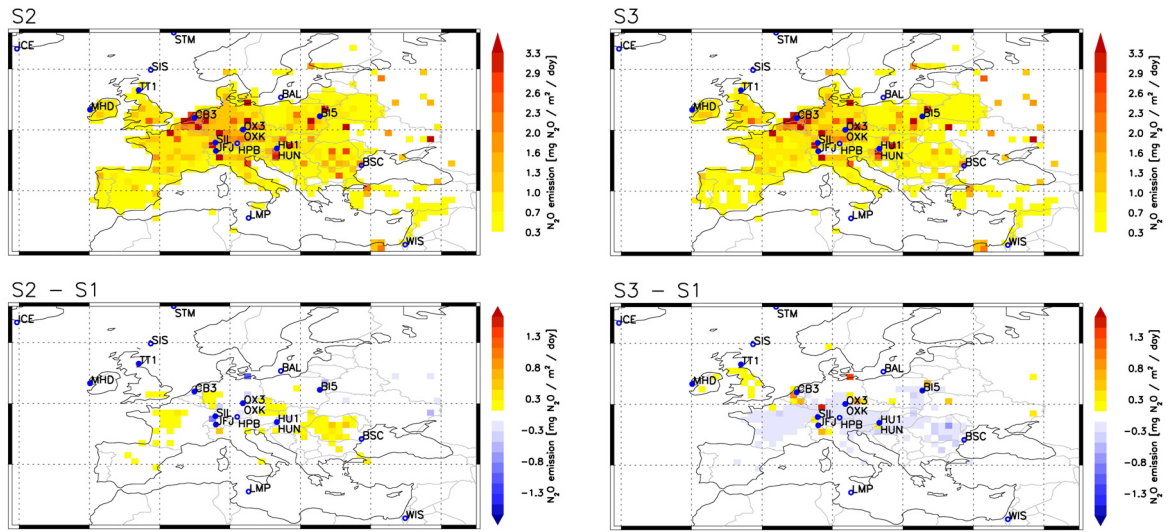
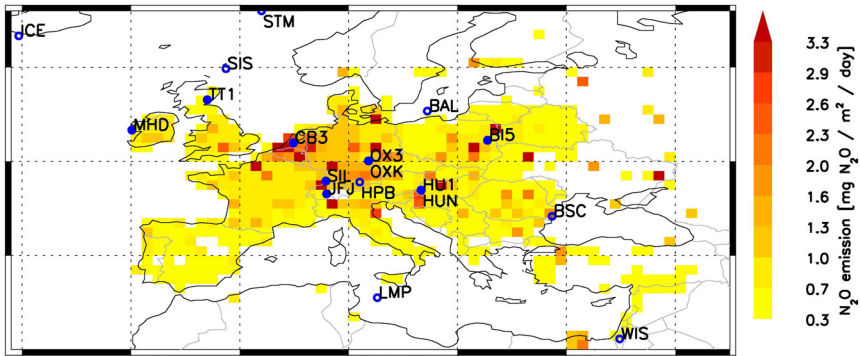


Figure S-5

S4



S4 - S1

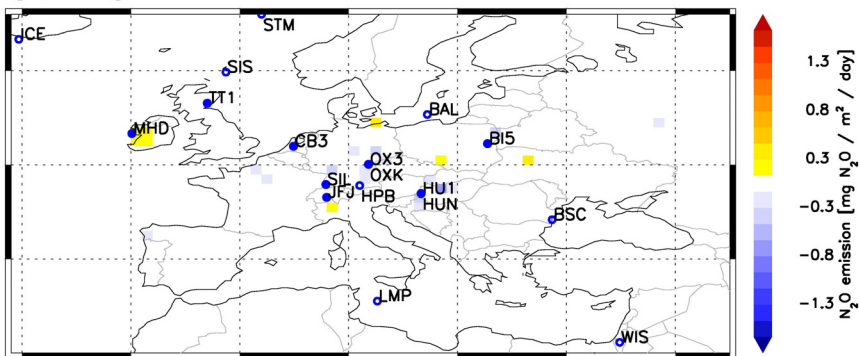


Figure S-6